

Electronic-structure effects in the suppression of superconductivity in hydrogenated Zr_2Rh

H. G. Salunke and G. P. Das*

Solid State Physics Division, Bhabha Atomic Research Centre, Bombay 400085, India

P. Raj, K. Shashikala, and A. Sathyamoorthy

Chemistry Division, Bhabha Atomic Research Centre, Bombay 400085, India

S. K. Dhar

Solid State Physics Group, Tata Institute of Fundamental Research, Bombay 400005, India

(Received 18 August 1995)

The observed suppression of superconductivity on hydrogenation of the $C16$ -structured intermetallic compound Zr_2Rh is explained qualitatively on the basis of the relationship between the electronic density of states at the Fermi level, the electron-phonon coupling constant, and T_c . The density of states at the Fermi level obtained from our local density electronic structure calculations has been compared with that estimated from low-temperature specific heat data. In pure Zr_2Rh , a relatively large superconducting transition temperature ($T_c \sim 11$ K) arises due to the Fermi level lying at the peak of the density of states, while in case of hydrogenated Zr_2Rh the lowering of T_c can be ascribed to the filling of bands and the shifting of the Fermi level either to a valley of the density of states (as in case of Zr_2RhH_2) or to a broad hump in the density of states (as in case of Zr_2RhH_4).

I. INTRODUCTION

The intermetallic compound Zr_2Rh has body-centered-tetragonal structure ($C16$ type, space group D_{4h}^{18}) and shows superconductivity below a transition temperature $T_c \sim 11$ K.^{1,2} This value of T_c for Zr_2Rh is one of the highest reported for noncubic binary systems, among conventional superconductors (i.e., excluding high-temperature oxide superconductors). Zr_2Rh , like the other compounds in the family, viz., Zr_2Fe (Ref. 3), Zr_2Co (Ref. 4), and Zr_2Ni (Refs. 5–7) is known to absorb a large quantity of hydrogen, about four to five hydrogen atoms per formula unit. The resulting ternary hydrides show a rich variety of changes in their electrical and magnetic properties.^{2,3}

In our recent experimental study,² the effect of hydrogen absorption on the structure, superconductivity, magnetic susceptibility, and low-temperature heat capacity of Zr_2Rh was investigated. It was shown that (i) $C16$ -type structure is retained on hydrogen absorption; (ii) although the hydride, like the parent intermetallic compound, exhibits metallic behavior, its superconducting transition temperature is greatly suppressed ($T_c < 2$ K); (iii) the hydride is also paramagnetic, but its susceptibility is reduced to almost half the value of Zr_2Rh ; and (iv) the electronic specific heat coefficient (γ) is reduced by almost an order of magnitude on hydriding. This study of Zr_2RhH_x was confined to a single composition, viz., $x=4.25$. Our subsequent experiments on the same system have now revealed that the actual composition of our sample in Ref. 2 was $x \approx 2.0$. This has been found to be due to the inadequacy of the normal surface poisoning procedure adopted earlier³ (resulting in partial hydrogen desorption) for the preparation of Zr_2Rh hydrides. It may be stressed that the composition Zr_2RhH_x ($x \approx 2$) is found to be relatively more stable (irrespective of any stabilization procedure) and

no appreciable loss of hydrogen takes place, as confirmed by x-ray studies at least over 2–3 months. It should also be emphasized that there is no qualitative change in the conclusions drawn from Ref. 2 as regards the effect of hydrogen absorption on all the properties studied except that the Debye temperature (Θ_D) was somewhat overestimated. The present work encompasses the compositions $x=0, 2$, and 4. In addition to the experimental studies on the hydrogen absorption characteristics of $C16$ -type intermetallics, we have also recently reported⁸ electronic structure calculations on pure Zr_2M compounds ($M = Fe, Co, Ni, \text{ and } Rh$). This study has revealed a systematic trend with regard to the role of $\rho(E_F)$, the density of states (DOS) at the Fermi level (E_F), on the observed T_c variation in these compounds. As the electron-to-atom ratio increases from 5.33 (for Zr_2Fe) to 5.67 (for Zr_2Co and Zr_2Rh) and further to 6.00 (for Zr_2Ni), E_F shifts from a valley to a peak and again into a next valley of the DOS. This band filling process, which gives rise to a change in $\rho(E_F)$, also results in a change in the electron-phonon coupling constant λ and a concomitant variation in T_c .

It would be interesting to know whether similar band filling effects can be expected when the change in the electron-to-atom ratio is brought about by hydrogen absorption. This has motivated us to carry out the present experimental investigations on these hydrogenated compounds, as well as first principles electronic structure calculations on modeled Zr_2RhH_x for $x=0, 2$, and 4. Section II deals with experimental details and in Sec. III we give a modeled structure of these compounds. In Sec. IV we discuss the results of our local density calculations and finally we give concluding remarks in Sec. V.

II. EXPERIMENTAL DETAILS

The procedure adopted for the preparation of Zr_2Rh and its hydrides as well as the estimation of structural and low-

TABLE I. Structural information used in our calculation.

Compound	a (Å)	c/a	vol/formula unit (Å ³)	W (Å)	R_{Zr}/W	R_{Rh}/W	R_{H}/W	R_E/W
Zr ₂ Rh	6.530	0.862	60.006	1.684	1.000	1.000	-	-
Zr ₂ RhH ₂	6.810	0.822	64.901	1.458	1.230	1.070	0.300	-
Zr ₂ RhH ₄	6.867	0.819	66.342	1.256	1.387	1.350	0.280	0.480

temperature heat capacity parameters has been described earlier.² Special care was taken to stabilize the highest hydrogen concentration, viz., Zr₂RhH_{*x*} (*x*~4) sample. Carbon monoxide at about 10 atm pressure was used for poisoning the hydride surface instead of oxygen; more importantly, hydrogen content was also estimated after completing the experiments, both by complete decomposition as well as by an x-ray cell parameter estimation. Heat capacity measurements on the *x*~4 composition could not be carried out below 7 K due to some problems with our experimental setup. However, magnetization measurements performed down to 2 K using a superconducting quantum interference device (SQUID) magnetometer revealed that Zr₂RhH_{*x*} (*x*~4) does not superconduct for temperatures above 2 K. The magnitude of molar susceptibility for the *x*~4 sample was found to be approximately 2.1×10^{-4} as compared to 3.7×10^{-4} for *x*=0 and 1.8×10^{-4} for *x*=2. The cell parameters for Zr₂RhH_{*x*} (*x*=0, 2, and 4) are given in Table I. The corresponding values of T_c , γ , and Θ_D derived from our heat capacity measurements are given in Table II.

III. MODELED STRUCTURE OF Zr₂RhH₂ AND Zr₂RhH₄

The arrangement of the atoms for C16-structured Zr₂Rh (Refs. 2,8–10) is schematically shown in Fig 1. It consists of planes of Zr atoms connected by Rh chains. The consecutive Zr planes are rotated by 45° with respect to each other. The C16 structure of these Zr₂M intermetallics permits the occupancy of four types of tetrahedral interstitial holes. The sites designated as *A* and *B* types have 4Zr, *C* type have (3Zr + 1M) and *D* type have (2Zr+2M) atoms at the vertices of the tetrahedral interstices. (See Ref. 6 for the nomenclature of different interstitial sites.) Although H-site occupancies have not been reported for the Zr₂RhH_{*x*} system, some neutron diffraction data on the site occupancies are available for isostructural deuterides, viz., Zr₂CoD_{4.8} (Ref. 4) and Zr₂NiD_{*x*} (*x*~2, 3, and 4.8) (Ref. 5). Furthermore, as in most hydride systems, the most probable H-site occupancy can be conjectured from the widely accepted guidelines;^{11,12} viz., (i) for an interstitial site to be

occupied, its hole radius should be ≥ 0.4 Å and the site with a bigger void size should get filled first, and (ii) the minimum distances between two hydrogen atoms should be ≥ 2.1 Å. Based on these guidelines, appropriate for the Zr₂RhH_{*x*} system and the experimental reports on related systems, we have assumed the occupancy of *B*-type tetrahedral sites for Zr₂RhH₂ and *C*-type sites for Zr₂RhH₄, for our electronic structure calculations. This is justified because in Zr₂NiD₂ it is known⁵ that deuterium atoms are almost exclusively on *B*-type sites, and in Zr₂CoD_{4.8}, four D atoms are reported⁴ to occupy *C*-type sites (data for lower D content in Zr₂CoD_{*x*} do not exist). There is some difference in the reported site occupancies for D atoms in Zr₂CoD_{4.8} (Ref. 4) as compared to Zr₂NiD_{4.8} (Ref. 5), although in both cases *C*-type sites are predominantly occupied. Our choice of site occupancy finds further support in the similarity of trends between the calculated and the experimental values of $\rho(E_F)$ obtained from the heat capacity measurements for the Zr₂RhH_{*x*} system, as discussed in the next section. The unit cells of Zr₂Rh, Zr₂RhH₂, and Zr₂RhH₄ contain 12, 20, and 28 atoms, respectively. The lattice parameters used in our calculations are the room temperature values as given in Table I. The use of room temperature lattice parameters for our 0 K band calculation causes a less than 1% error, which is within the error bar of the method discussed below.⁸

IV. RESULTS AND DISCUSSIONS

A. Electronic structure

As in our earlier local density calculations on pure C16-structured intermetallics,⁸ we have deployed the tight-binding linear muffin tin orbital within atomic sphere approximation^{13,14} (TB-LMTO-ASA) method and using von Barth–Hedin parametrization¹⁵ for the exchange-correlation potential. In this method, one uses space filling (and hence slightly overlapping) atomic (Wigner-Seitz) spheres centered around each site in the unit cell. While in the case of Zr₂Rh we had chosen⁸ equal sphere radii for constituent metals, for the hydrogenated compounds we use smaller

TABLE II. Specific heat and local density approximation (LDA) data for Zr₂Rh and its hydride.

C16 compounds	Experimental heat capacity data				LDA calculation	
	T_c (K)	γ (mJ/mol K ²)	Θ_D (K)	λ (est)	$N(E_F)$ (est) (states/eV f.u.)	$N(E_F)$ (states/eV f.u.)
Zr ₂ Rh	11.2	68.0	214	1.13	6.77	5.40
Zr ₂ RhH ₂	<2.0	6.5	350	<0.49	<1.0	1.2
Zr ₂ RhH ₄	<2.0	21.0	371	<0.49	<3.0	2.7

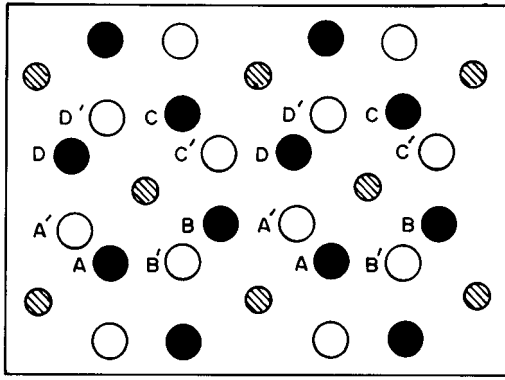


FIG. 1. Atomic arrangement of Zr and Rh atoms in Zr_2Rh : Solid circles denote Zr atoms at $z=0$, and open circles denote Zr atoms at $z=\pm 1/2$, while hatched circles denote Rh atoms at $z=\pm 1/4$.

spheres around the hydrogen atoms in the above-mentioned model. This ensures reasonable sphere overlaps, which are essential for the LMTO-ASA method to work satisfactorily. The compound Zr_2RhH_4 required “empty spheres”,¹⁴ to be placed in interstitial sites designated as A (Ref. 6) for reasonable sphere overlaps. The ratio of the individual atomic sphere radii to the average sphere radius, R/W , for the three structures studied is given in Table I. We have used s , p , and d partial waves for the Zr and Rh atoms, while for hydrogen we have *downfolded*¹⁶ the p partial waves (hydrogen d orbitals have not been included in the basis). We have also included the so-called “combined correction” term in our calculations. The resulting DOS’s are shown in Figs. 2 and 3, respectively.

The DOS’s for all the three compounds (Fig. 2) have a “teethed structure” which is typical of transition metals. The value of DOS at E_F for Zr_2RhH_2 is smaller as compared to that for Zr_2RhH_4 . A comparison of DOS’s for the three structures shows that the Fermi level shifts from the peak to the valley while going from Zr_2Rh to Zr_2RhH_2 and again to the neighboring broad hump for Zr_2RhH_4 . This shifting of E_F across the peaks and valleys of DOS has also been observed in pure Zr_2M ($M=Fe, Co, Ni$, and Rh) intermetallics.⁸ There appears to be a compression in the DOS for hydrogenated Zr_2Rh as compared to the pure intermetallic, suggesting that the states which were above E_F for pure Zr_2Rh are “pulled” down below E_F for the hydrogenated compound, thereby implying a filling up of bands upon hydrogenation. One may conjecture such a band filling as resulting from a possible transfer of electrons from the hydrogen s state to the unoccupied valence state of Zr_2Rh . The partial electronic charges within the Zr, Rh, H, and empty spheres, as coming out from our self-consistent calculations, are enlisted in Table III. The total number of valence electrons per “formula unit” (containing one Rh and two Zr spheres) are found to be 17, 18.32, and 20.07 in Zr_2Rh , Zr_2RhH_2 , and Zr_2RhH_4 , respectively. This qualitatively supports our charge transfer conjecture, although it is hard to quantify this within the atomic sphere approximation. In this context, one may study the partial DOS’s on transition metal sites (Fig. 3), which also contain “tails” of the hydrogen s orbital protruding into the Zr and Rh spheres. The new

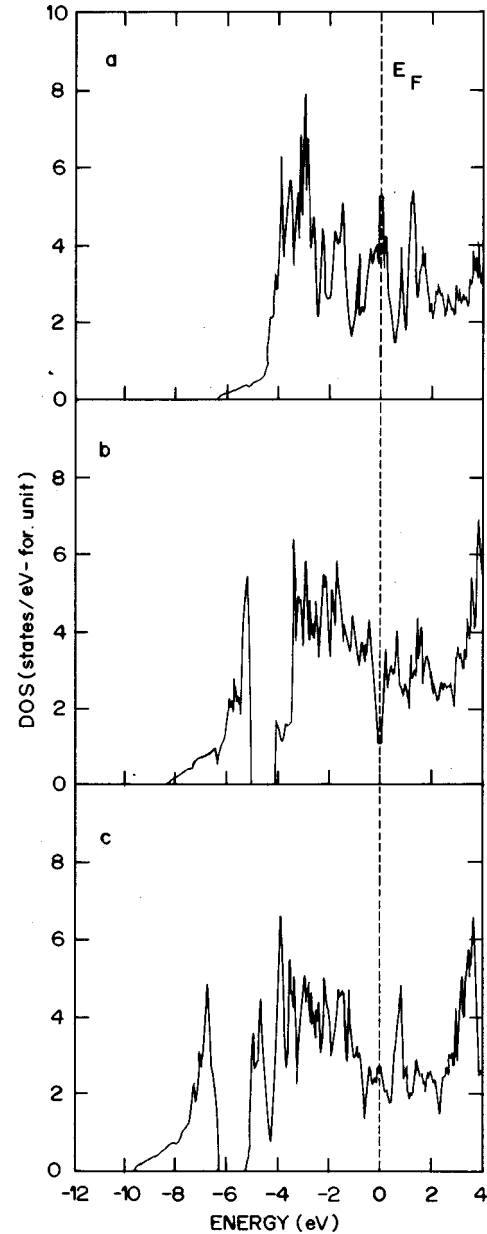


FIG. 2. Total electronic density of states for (a) Zr_2Rh , (b) Zr_2RhH_2 , and (c) Zr_2RhH_4 .

DOS peaks appearing between -6 and -10 eV in the hydrogenated compounds carry this signature. Also it is clear that the magnitudes of $\rho(E_F)$ for Zr and Rh spheres are comparable, implying that these compounds are not “chain superconductors”,¹⁷ — a result similar to that observed for the pure intermetallics.⁸ Here it may be mentioned that the calculated variation of $\rho(E_F)$ as the H content increases in going from Zr_2RhH_2 to Zr_2RhH_4 is different from the trend inferred by Aubertin *et al.*¹⁸ for the Zr_2NiH_x system. From pulsed proton nuclear magnetic resonance measurements, these authors derived the Korringa constant values as a function of hydrogen concentration x , and concluded that $\rho(E_F)$ increases monotonically with an increase in x . The value of the DOS at E_F has an important consequence on the superconducting properties of these compounds, as we shall see in the next section.

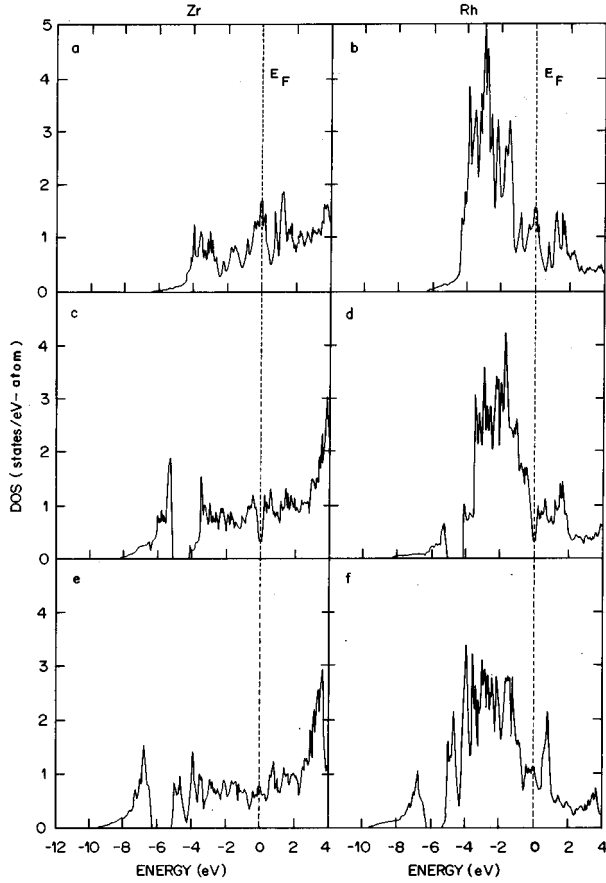


FIG. 3. Site-projected density of states on the Zr site and Rh site for Zr_2Rh [(a) and (b)], Zr_2RhH_2 [(c) and (d)], and Zr_2RhH_4 [(e) and (f)].

B. Superconductivity

For a complete *ab initio* study of the superconducting properties, one requires, along with the electronic structure, information on the phonon dispersion in these compounds.¹⁹ However, due to lack of information on phonon dispersions, we have made a comparative study of the superconducting properties employing a procedure similar to that used for pure Zr_2M ($M = Fe, Co, Ni,$ and Rh) compounds.^{8,19} We compare in this procedure the $\rho(E_F)$ calculated from first principles with that estimated from specific heat measurements. Figure 4 gives specific heat curves for the three compounds. Unlike Zr_2Rh which distinctly shows a discontinuity at $T_c = 11.2$ K, the specific heat measurement for Zr_2RhH_2 and Zr_2RhH_4 show a monotonic decrease with decreasing temperature. The electronic specific heat coefficient (γ) and Debye temperature (Θ_D) derived from these curves are listed in Table II. A point to note is a relatively larger γ in the case of Zr_2RhH_4 than Zr_2RhH_2 , although

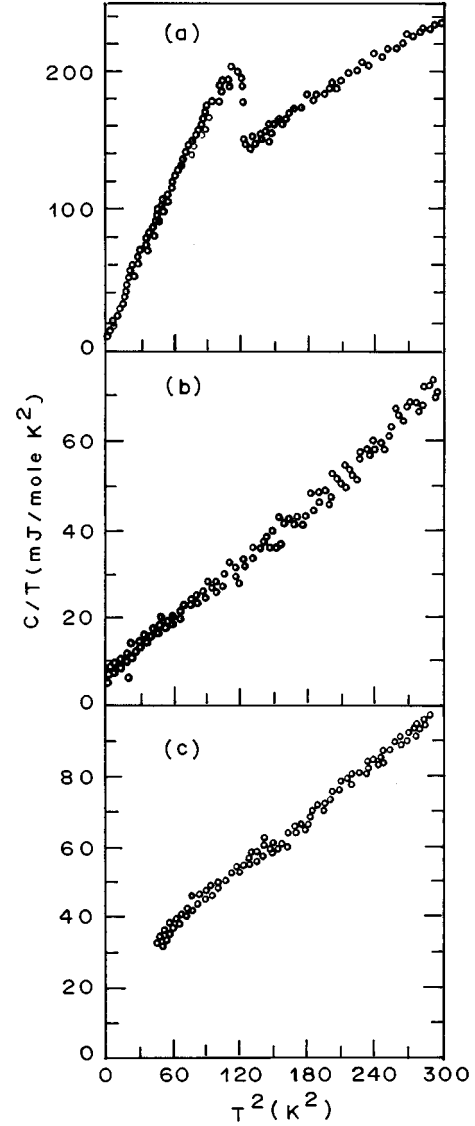


FIG. 4. Temperature dependence of heat capacity for (a) Zr_2Rh , (b) Zr_2RhH_2 , and (c) Zr_2RhH_4 in the form C/T vs T^2 . The data for Zr_2RhH_4 are shown only up to ~ 7 K (although the experiment was performed up to 2 K) because of sample calibration errors. (Also see Ref. 2.)

both these compounds have close Θ_D values. This information from specific heat measurements is used in Macmillan's formula^{19,20} for superconducting T_c , in order to estimate λ . This value of λ in turn is used in a modified Sommerfeld's expression for the electronic specific heat, viz., $\gamma = \frac{2}{3}\pi^2 k_B^2 \rho(E_F)(1 + \lambda)$, to arrive at an estimate of $\rho(E_F)$. In Table II we show a comparison of this estimated $\rho(E_F)$ from specific heat data with the first principles LDA calculations.

TABLE III. Partial charges within the atomic spheres in pure and hydrogenated Zr_2Rh .

	Zr sphere			Rh sphere			H sphere		Empty sphere	
	Q_s	Q_p	Q_D	Q_s	Q_p	Q_D	Q_s	Q_p	Q_s	Q_p
Zr_2Rh	0.581	0.608	2.428	0.942	0.786	8.038	-	-	-	-
Zr_2RhH_2	0.688	1.019	2.951	0.717	0.626	7.657	0.338	0.004	-	-
Zr_2RhH_4	0.657	1.063	3.200	0.853	1.179	8.201	0.191	0.002	0.140	0.015

It is observed that the calculated values follow a similar trend as the estimated ones. This implies that Zr_2RhH_x ($x=0, 2, 4$) follows a similar band filling prescription as was observed in the case of Zr_2M ($M=Fe, Co, Ni, \text{ and } Rh$) intermetallics.⁸

V. CONCLUSIONS

First principles local density band calculations using the TB-LMTO-ASA method have been performed on modeled C16-structured Zr_2RhH_x compounds, in order to understand the decrease in superconducting T_c on hydrogenation. The calculated DOS at the E_F can be related to the electronic specific heat via the electron-phonon coupling constant. The measured quantities (γ , θ_D , and T_c) from our low-temperature specific heat experiment have been used to determine λ , which in turn yields an estimate of $\rho(E_F)$. We

have compared this with the LDA value of $\rho(E_F)$, and found that on hydrogenation the Fermi level shifts from the peak of the DOS (for Zr_2Rh) to either one of the valleys of the DOS (for Zr_2RhH_2) or to a broad hump (for Zr_2RhH_4). In order to get a completely first principles estimate of λ and hence T_c , one must evaluate the average squared phonon frequencies from the detailed phonon dispersion spectrum which is *not* available for these compounds. In this paper we have been able to arrive at a qualitative understanding of the trend in the T_c values in terms of band filling and consequent variation of $\rho(E_F)$ in Zr_2Rh and its hydrides.

ACKNOWLEDGMENTS

We would like to thank Dr. V.C. Sahni and Dr. B.A. Dasannacharya for helpful discussions and for their encouragement in this work.

*Electronic address: gpd@magnum.barct1.ernet.in

¹R. Kuentzler and R.M. Waterstrat, *Solid State Commun.* **54**, 517 (1985).

²P. Raj, P. Suryanarayana, A. Satyamoorthy, K. Shashikala, R.M. Iyer, S.K. Dhar, L.C. Gupta, V.C. Sahni, and R.J. Begum, *J. Alloys Compounds* **206**, 47 (1994).

³P. Raj, P. Suryanarayana, A. Satyamoorthy, K. Shashikala, and R.M. Iyer, *J. Alloys Compounds* **178**, 393 (1992).

⁴F. Bonhomme, K. Yvon, and M. Zolliker, *J. Alloys Compounds* **199**, 129 (1993).

⁵A. Chikdene, A. Baudry, P. Boyer, S. Miraglia, D. Fruchart, and J.L. Soubeyroux, *Z. Phys. Chem. (München)* **163**, 219 (1989).

⁶P. Boyer and A. Baudry, *J. Alloys Compounds* **129**, 213 (1987).

⁷K. Shashikala, N.M. Gupta, P. Suryanarayana, A. Satyamoorthy, V.S. Kamble, and P. Raj, *J. Mol. Catalysis* **91**, 223 (1994).

⁸H.G. Salunke, G.P. Das, P. Raj, V.C. Sahni, and S.K. Dhar, *Physica C* **226**, 385 (1994).

⁹F.R. Eshman and J.F. Smith, *J. Appl. Phys.* **46**, 5080 (1975).

¹⁰R. Visnov, F. Ducastelle, and G. Treglia, *J. Phys. F* **12**, 441 (1982).

¹¹D.G. Westlake, *J. Less Common Met.* **90**, 251 (1983).

¹²A.C. Switendick (unpublished).

¹³O.K. Andersen and O. Jepsen, *Phys. Rev. Lett.* **53**, 2571 (1984).

¹⁴O.K. Andersen, O. Jepsen, and M. Sob, in *Electronic Band Structure and Its Applications*, edited by M. Yussouff (Springer-Verlag, Berlin, 1987), p. 1.

¹⁵U. von Barth and L. Hedin, *J. Phys. C* **5**, 1629 (1972).

¹⁶M. van Schilfgarde, A.T. Paxton, O. Jepsen, and O.K. Andersen (unpublished).

¹⁷S.K. Sinha and B.N. Harmon, *Phys. Rev. Lett.* **35**, 1515 (1976).

¹⁸F. Aubertin, S.J. Campbell, J.M. Pope, and U. Gonser, *J. Less Common Met.* **129**, 297 (1987).

¹⁹H.L. Skriver and L. Mertig, *Phys. Rev. B* **32**, 4431 (1985).

²⁰I.I. Mazin, S.N. Rashkeev, and S.Y. Savrasov, *Phys. Rev. B* **42**, 366 (1990).